A Comprehensive CFD Model for the Biomass Pyrolysis

Giancarlo Gentile*, Alberto Cuoci, Alessio Frassoldati, Tiziano Faravelli, Eliseo Ranzi

Politecnico di Milano; Dipartimento di Chimica, Materiali e Ingegneria Chimica “Giulio Natta”, Piazza Leonardo Da Vinci, 32; 20133 Milano; Italia
giancarlo.gentile@polimi.it

1. Introduction

The need for energy sources differentiation is one of the most important challenges that the scientific community will have to solve in the next years. Fossil fuels cover more than 75% of the primary energy consumption, and such a condition cannot be accepted in a long-term scenario. In this context, biomass represents a domain of growing interest and development. It is important, consequently, to spend modeling efforts in the direction of a clearer and deeper understanding of biomass characterization, in order to develop and address the technological implementation of processes for the effective exploitation of biomass potential.
The comprehensive description of the thermal degradation of biomass materials is a very complex and challenging subject. It includes several levels of consideration and modeling since it is a multi-component, multi-phase and multi-scale problem. Consequently, an accurate description of the overall system is crucial for a deeper understanding of the global process. A lot of modeling effort have been performed in the last years, in order to provide better insight into this system, many of them involving theoretical approaches combined with experimental data. Furthermore, this analysis of the biomass particle can be directly extended and used also for coal gasification and combustion.
In this work a new solver for OpenFOAM® (OpenFoam, 2011), named bioSMOKE, was developed with the aim to efficiently perform CFD simulations at the particle scale for very complex 3D geometries with detailed kinetic schemes that allow the correct trade-off between numerical accuracy e computational costs. The devolatilization of the biomass is considered a straightforward combination of the pyrolysis of three reference components: cellulose, hemicellulose, and lignins as already discussed elsewhere (Ranzi et al., 2008). The multistep kinetic scheme used in current study is the POLIMI_BM_1402 (Corbetta et al., 2014) that describe the pyrolysis of the biomass through 42 species and 24 reactions.
In this preliminary implementation the shrinking of the porous medium, as well as the gas phase reactivity, are neglected and only the transport phenomena inside the biomass particle are take into account.

The paper is structured as follows. In Section 2, we provide a detailed description of the governing equations at the particle scale with a comprehensive detail of the numerical method and its applications with OpenFOAM®. In the Section 3, we provide the validation of the code and present a showcase of pyrolysis of a pellet of poplar wood in order to validate the method and to test reliability and efficiency of the new solver.

2. Mathematical formulations

The mathematical model for the biomass pyrolysis is based on the fundamental governing equations of conservations of total mass, momentum and energy for both gaseous and solid phases. The latter is considered as a porous medium including both the solid volume and the fluid contained inside its pores.

2.1 Governing equations

The porosity within the particle is determined as follows (Eq. (1)) in order to estimate the effective solid and gaseous volume in every computational cell.

$$\varepsilon(t) = 1 - \frac{m^S(t)}{\rho^S V} \tag{1}$$

$m^S(t)$ is the total mass of solid, ρ^S is the solid density, V is the total particle volume.

$\varepsilon = 0$ when only the solid phase is present and $\varepsilon = 1$ if there is no solid.

The equation used for conservation of mass for the gas phase is written as (Eq. (2)):

$$\frac{\partial}{\partial t}\left(\rho^G \varepsilon\right) + \nabla\left(\rho \mathbf{u}\right) = \dot{\Omega} \tag{2}$$

ρ^G is the gas density, while $\mathbf{u}$ is the velocity field. The source term $\dot{\Omega}$ represents the total mass added in the gas phase through the pyrolysis reactions that take place in the solid volume.

The equation for conservation of momentum is given by Eq. (3)

$$\frac{\partial}{\partial t}\left(\rho^G \varepsilon \mathbf{u}\right) + \nabla\left(\rho^G \mathbf{u}\mathbf{u}\right) = -\nabla p + \nabla \cdot \left[\mu\left(\nabla \mathbf{u} + \nabla \mathbf{u}^T\right) - \frac{2}{3}\mu\left(\nabla \mathbf{u}\right)\mathbf{I}\right] + \rho \mathbf{g} + \mathbf{S} \tag{3}$$

p is the static pressure, $\rho \mathbf{g}$ is the gravitational body force and $\mathbf{S}$ is a source term computed according the Darcy-Forchheimer Law Eq. (4)

$$\mathbf{S} = -\left(\mu \mathbf{D} + \frac{1}{2}\rho^G \left|u_{kk}\right| \mathbf{F}\right)\mathbf{u} \tag{4}$$

μ is the molecular viscosity, while $\mathbf{D}\left[m^{-2}\right]$ and $\mathbf{F}\left[m\right]$ are the Darcy and Forchheimer constants, respectively.

$\mathbf{S}$ is composed of two terms, a viscous loss term and an inertial loss term, creating a pressure drop that is proportional to the velocity and velocity squared, respectively.

The gas and solid species conservation equations are shown in Eqs. (5-6).

$$\frac{\partial}{\partial t}\left(\rho^G \varepsilon \omega_k\right) + \nabla\left(\rho^G \omega_k \mathbf{u}\right) = -\nabla j_k + \dot{\Omega}_k \qquad k = 1, ..., NC_{gas} \tag{5}$$

$$\frac{\partial}{\partial t}\left(\rho^S \left(1-\varepsilon\right)\omega_j\right) = \dot{\Omega}_j \qquad j = 1, ..., NC_{solid} \tag{6}$$

ρ^S is the solid density, j_k are the diffusion fluxes computed according the Fick's Law, $\dot{\Omega}_k$ and $\dot{\Omega}_j$ are the reaction rates for the gas and solid species, respectively. NC_{gas} and NC_{solid} are the total number of gas and solid species.

Conversely, the energy equation is solved by Eq. (7) assuming a thermal equilibrium between solid and gas phase.

$$\hat{C}_p^{gas}\frac{\partial\left(\rho_g \varepsilon T\right)}{\partial t} + \hat{C}^{solid}\frac{\partial\left(\rho^S\left(1-\varepsilon\right)T\right)}{\partial t} + \hat{C}_p^{gas}\nabla\left(\rho_g \mathbf{u} T\right) = -\nabla q - \left.\frac{\partial \ln \rho^G}{\partial \ln T}\right|_p \frac{Dp}{Dt} + \dot{Q}_R - \sum_{k=1}^{NC_{gas}} \hat{H}_k \nabla j_k \tag{7}$$

$\hat{C}_p^{gas}$ is the specific heat at constant pressure for the gas mixture, $\hat{C}^{solid}$ is the solid specific heat, T is the temperature field, q is the conductive flux computed according the Fourier's Law, $\frac{Dp}{Dt}$ is the pressure substantial derivative, $\dot{Q}_R$ is the reaction heat.

2.2 Numerical method

The numerical scheme adopted exploits the operator-splitting technique to solve this system. The governing equations are split in two sub-equations, the transport and the reactive term as discussed by (Maestri and Cuoci, 2013). The bioSMOKE solver is based on the algorithm used in the standard OpenFOAM® framework for compressible, unsteady, laminar and turbulent flow. In particular the PIMPLE (PISO-SIMPLE) algorithm was modified in order to implement the operator splitting technique. A similar approach was already applied by (Cuoci et al., 2013) for the numerical simulation of laminar coflow flames.

3. Results and discussion

In this section we provide validation tests in order to verify the reliability of the new CFD tool developed. First of all, the simple heating of a ceramic cylinder was analyzed in order to test the consistency of the computational grid, minimizing the computational effort that would be required by reactive simulations. After that a reactive test was performed for the devolatilization and pyrolysis of dried beech wood.

3.1 Heating test

Since the pyrolysis is a thermal process, a simple preliminary test of heating a ceramic cylinder was carried out. The results of the simulation were be compared with experimental data collected by (Gauthier, 2013).
The computational mesh adopted (25280 cells, height = 3 cm, diameter = 2 cm) is shown in Figure 1, while the simulation parameters are reported in Table 1.

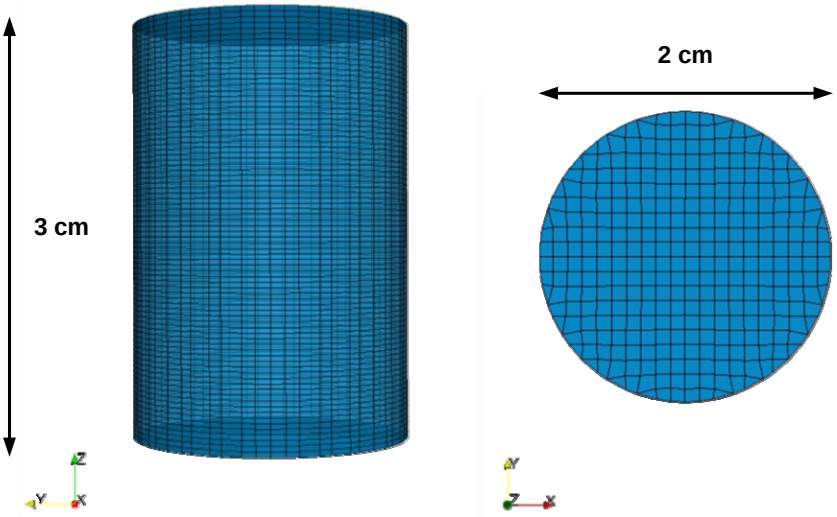

Figure 1: 3D computational mesh used for the simulation in the y-z plane (left) and x-y plane (right) with detail about the geometry

Table 1: Ceramic physical properties

Density [kg/m^3]	Thermal conductivity [W/m/K]	Specific Heat [J/kg/K]
850	$1.97\cdot10^{-1} + 3.91\cdot10^{-5}\cdot T + 2.03\cdot10^{-8}\cdot T^2$	960

The ceramic cylinder, originally at room temperature, was placed within an oven, named PYRATES as described by (Gauthier, 2013). The heat exchange occurs for radiation with a radiant wall temperature set to 800 °C. A thermocouple was placed in different positions along the radial coordinate of the cylinder in order to measure the local value of temperature during the transient. Radial temperature profiles are reported in Figure

2. The cylinder reaches a uniform temperature at about 400 s. Figure 3 shows the comparison between model and experimental trend for the temperature measured in three different radial coordinates along the section of the cylinder. The predictions of the new code agree very well with the experimental data.

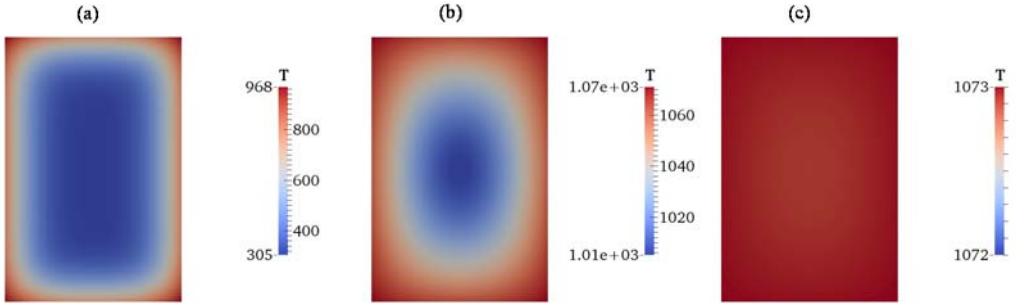

Figure 2: Cross-section temperature profile in the centre of the cylinder (x=0) for different times. Panel a: 10 s, panel b: 200 s, panel c: 600 s. Temperature [K]

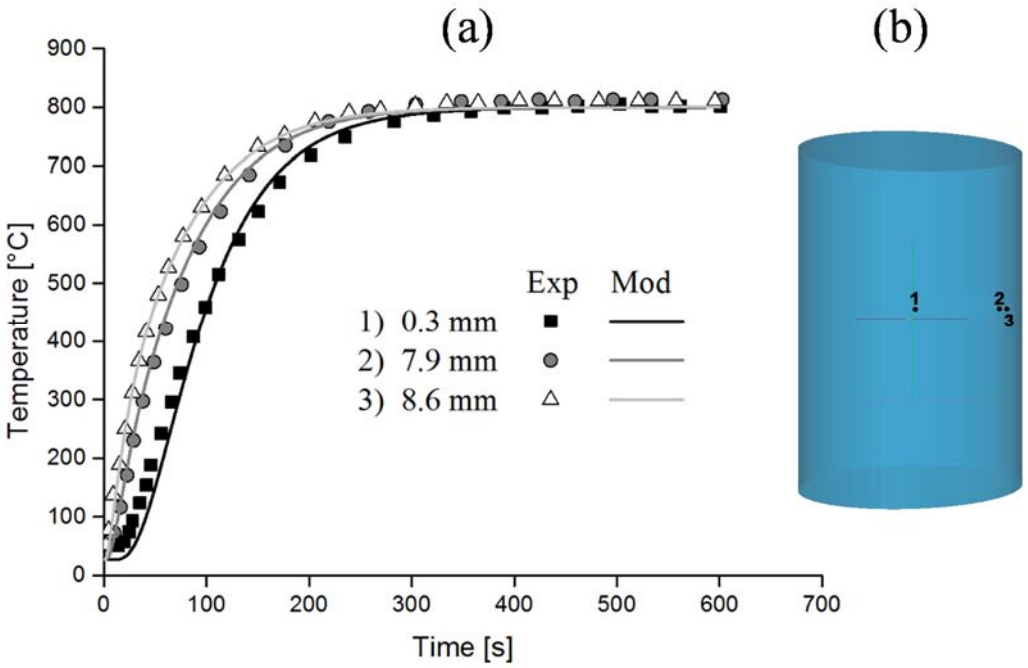

Figure 3: Temperature profiles within the ceramic cylinder at z=1 mm and r= 0.3-7.9.8.6 mm (Panel a). Panel b shows the effective position of the thermocouple during the heating of cylynder.

To emphasize the potentiality of this 3D solver, the heating of the ceramic cylinder was simulated setting non-uniform temperature conditions at the domain boundaries. In particular the lateral surface of the cylinder was split in two parts and different Neumann boundary conditions were specified for the temperature field, as shown in Figure 4.

Temperature profiles are shown in Figure 5 during the transient. Unlike the previous case, a non-symmetric temperature distribution is observed with strong variations between corners and edges subject to different boundary conditions. Of course, the cylinder reaches the same final temperature in steady-state condition (t= 700 s). The effective temperature distribution within the solid particle is a very important issue to take into account in the modeling of thermal processes like the pyrolysis is. In this respect, 1D or 2D models cannot distinguish between such local deviations, and thus, this example provides compelling evidences of the potentiality and feasibility of the new 3D numerical code developed.

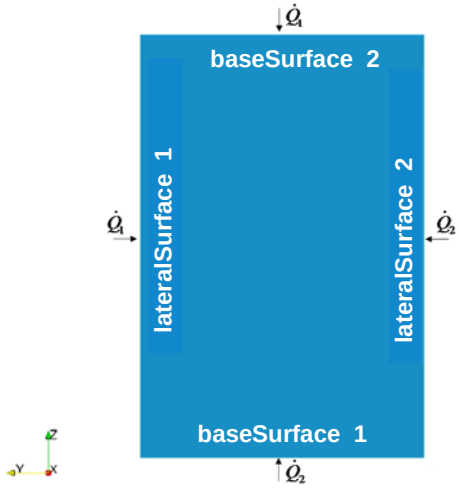

$$\dot{Q}_1 = \sigma \cdot \varepsilon \cdot \gamma \cdot \left(T_w^4 - T^4 \right)$$

$$\dot{Q}_2 = \frac{1}{3} \dot{Q}_1$$

$$\sigma = 5.67 \cdot 10^{-8} \frac{W}{m^2 \cdot K^4}$$

$$\varepsilon = 0.9 \; ; \; \gamma = 1 \; ; \; T_w = 800°C$$

Figure 4: Cross-section computational domain in the y-z plane

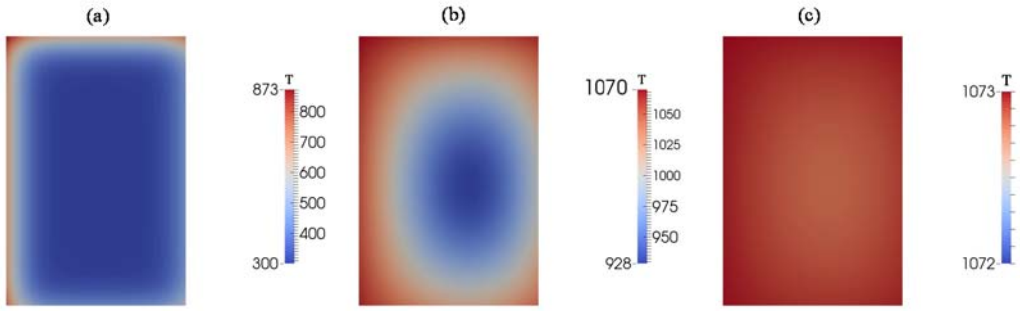

Figure 5: Cross-section temeprature profile in the centre of the cylinder (x=0) for different times. Panel a: 10 s, panel b: 200 s, panel c: 700 s. Temperature [K].

3.2 Reactive test: pyrolysis of woody biomass

The pyrolysis simulation of a beech wood biomass was carried out for the same geometry presented above. This show case represents an ideal benchmark for the new solver because the pyrolysis occur under "thermally thick" conditions with strong internal temperature gradients during the devolatilization. The operating conditions of the simulation are reported in Table 2.

Table 2: Operating conditions for biomass cylinder

Operating conditions	
Inlet temperature [K]	300
Surface temperature [K]	750
Inlet pressure [Pa]	101325
Height [cm]	3
Diameter [cm]	2
Inlet porosity [-]	0.176
Inlet mass fraction [%]	
Cellulose	47
Hemicellulose	25.5
Lignin	26.7
Ash	0.8

Figure 6 shows a comparison between experimental data (Gauthier et al., 2013) and predicted profiles of centre temperature. In these conditions both the kinetics and the heat transfer operate on comparable timescales and the new CFD code is able to describe the combined effect of chemical kinetic and transport phenomena with a good agreement with the experimental trend. The profiles show the presence of two thermal regimes during wood pyrolysis. Temperature first increases until reaching an inflexion point respectively at about 300 s. From this inflexion point, temperature strongly increases, even exceeding the steady state plateau. Similar results were already discussed by (Milosavljevic and Suuberg, 1995, Corbetta et al., 2014). They concluded that the endothermicity of the process mainly reflects the latent heat requirement for the pyrolysis reactions. In contrast, the exothermic character of char formation, which depends on the reaction conditions, is the reason for the occurrence of a maximum in centre temperature.

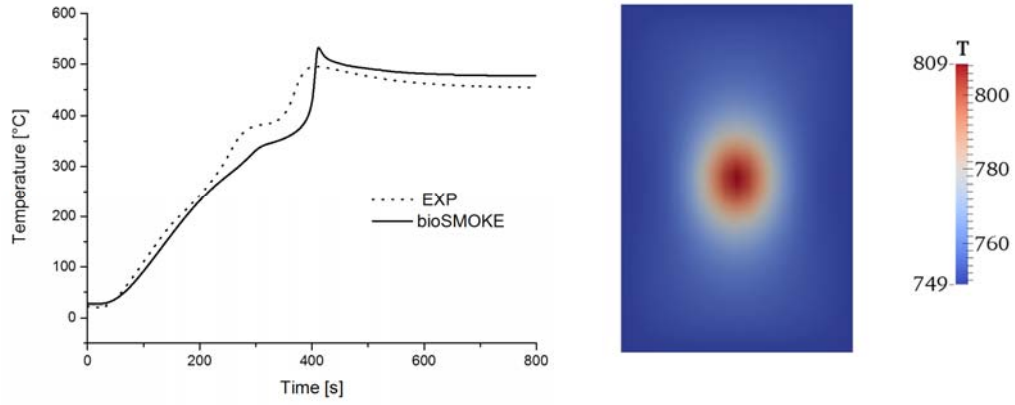

Figure 6: Temperature profile within the wood cylinder at r = 0 (left).Cross-section temeprature profile (x=0) at t= 420 s. Temperature [K] (right).

Conclusions

A general and comprehensive CFD model for the biomass pyrolysis has been developed in this preliminary work. It has been validated against different set of experimental data both in non-reactive conditions (simple heating of ceramic cylinder) and in presence of thick particle pyrolysis. The model turns to be in good agreement with the experimental trends and paves the way to be very useful in the modelling of thermochemical processes that involve solid particles. In particular, a key area of possible improvement is the study of the impact of particle shrinking during the devolatilization in respect of the evaluation of physically parameters such as particle size and porosity and the coupling with the CFD modeling of the gas-phase region surrounding the particle.

This work represents a first step towards the ultimate goal that is to better understand the complex behaviour of solid fuel pyrolysis and gas-solid interactions taking place in gasifiers reactors.

References

Corbetta, M., Frassoldati, A., Bennadji, H., Smith, K., Serapiglia, M. J., Gauthier, G., Melkior, T., Ranzi, E. & Fisher, E. M. 2014. Pyrolysis of centimeter-scale woody biomass particles: Kinetic modeling and experimental validation. *Energy and Fuels,* 28**,** 3884-3898.

Cuoci, A., Frassoldati, A., Faravelli, T. & Ranzi, E. 2013. A computational tool for the detailed kinetic modeling of laminar flames: Application to C2H4/CH4 coflow flames. *Combustion and Flame,* 160**,** 870-886.

Gauthier, G. 2013. *Synthése de biocarburants de deuxiéme génération: Etude de la pyrolyse à haute température de particules de bois centimétriques.* Ph.D., Université de Toulouse.

Gauthier, G., Melkior, T., Grateau, M., Thiery, S. & Salvador, S. 2013. Pyrolysis of centimetre-scale wood particles: New experimental developments and results. *Journal of Analytical and Applied Pyrolysis,* 104**,** 521-530.

Maestri, M. & Cuoci, A. 2013. Coupling CFD with detailed microkinetic modeling in heterogeneous catalysis. *Chemical Engineering Science,* 96**,** 106-117.

Milosavljevic, I. & Suuberg, E. M. 1995. Cellulose thermal decomposition kinetics: Global mass loss kinetics. *Industrial and Engineering Chemistry Research,* 34**,** 1081-1091.

Openfoam 2011. www.openfoam.com. Accessed 20.12.2014

Ranzi, E., Cuoci, A., Faravelli, T., Frassoldati, A., Migliavacca, G., Pierucci, S. & Sommariva, S. 2008. Chemical kinetics of biomass pyrolysis. *Energy and Fuels,* 22**,** 4292-4300.